

Research Article

Prediction of Pork Fatty Acid Content using Image Texture Features

^{1,2}Xin Sun, ¹David Newman, ¹Jennifer Young, ²Yu Zhang and ¹Eric Berg

¹Department of Animal Sciences, North Dakota State University, Fargo, ND 58102, USA

²Department of Engineering, Nanjing Agricultural University, Nanjing 210031, China

Abstract: The objective of this study was to investigate the usefulness of image texture features obtained from fresh (never frozen) pork backfat for the prediction of fatty acid content and Iodine Value (IV). Five image texture features (directionality, contrast, roughness, heterogeneity and line-likeness) were extracted from cross-sectional images of 9pork loin chops with overlying subcutaneous fat. Texture features were extracted from images obtained on the subcutaneous fat using a digital camera. A full fatty acid profile was determined for each subcutaneous fat sample using AOAC and AOCS official methods. Linear and stepwise regression methods were utilized to establish the prediction models for oleic, linoleic and linolenic fatty acids and IV. Linear regression analyses produced higher coefficients of determination (R^2) for all 3fatty acids. Linear regression models for linoleic and linolenic acid generated an R^2 of 0.95. These preliminary findings suggest potential for use of image texture features for prediction of pork fattyacid values and subsequent pork fat quality.

Keywords: Fatty acid, image processing, iodine value, prediction, texture feature

INTRODUCTION

For customer expectations, pork processors put an emphasis on belly quality quantified via Iodine Value (IV), an indicator of overall fat firmness. The IV provides processors a numeric estimate of the level of unsaturation in the cut of interest by reacting iodine compounds to the samples' C = C bonds (Hallenstvedt *et al.*, 2012). Besides iodine titration, IV can be calculated from the samples fatty acid profile (Cd 1c-85 AOCS, 1998). Both methods to determine IV are time consuming and destructive; therefore, a consistent and non-destructive method that could be applied in an automated online situation would be desirable to quantify fatty acid profile (fat quality) in real-time.

Computer vision techniques have been previously investigated as an objective method to monitor lean and fat quality (Chen *et al.*, 2010; Chmiel *et al.*, 2011a, 2011b; Girolami *et al.*, 2013). Furthermore, computer vision and image texture features have been used as method of evaluating lamb composition and quality (Chandraratne *et al.*, 2006a, 2007, 2006b). Sun *et al.* (2012) predicted beef tenderness using color and image texture features and (Sun *et al.*, 2014) recently published an image texture feature-based method to predict beef troponin-T post-mortem degradation product. These studies show the potential for image processing techniques to replace time consuming, expensive chemical methods of meat analyses.

The aim of this study was to investigate the analytical potential of computer image processing and texture analysis techniques to quantify fatty acids associated with soft pork (specifically oleic, linoleic, linolenic and IV). The specific objective was to develop a non-destructive, objective method to evaluate pork subcutaneous fatty acid parameters using image and texture features with two comparable regression models (linear and stepwise).

MATERIALS AND METHODS

Pork samples and fatty acid analysis: Fresh pork loins were obtained from 9pork sides used in a separate research project that compared feeding obese swine a diet containing 16% corn oil (VEG) or 36% beef tallow (ANIM). The 3mo feeding strategy resulted in significant differences in fatty acid profiles of the subcutaneous fat. The Iodine Value (IV) and concentration of oleic, linoleic and linolenic acid expressed as percentage of total fat in a sample of subcutaneous fat collected adjacent the 10th thoracic vertebra were 85.8 (± 5.1), 36.2 (± 2.8), 26.9 (± 3.6) and 2.4 (± 0.4)% for VEG and were 60.2 (± 3.5), 44.5 (± 1.7), 9.8 (± 1.2) and 0.6 (± 0.2)% for ANIM, respectively. The iodine value in this study was calculated as:

After a 24h chill (2°C), each pork carcass was fully quartered at the 10th/11th rib interface and the blade and

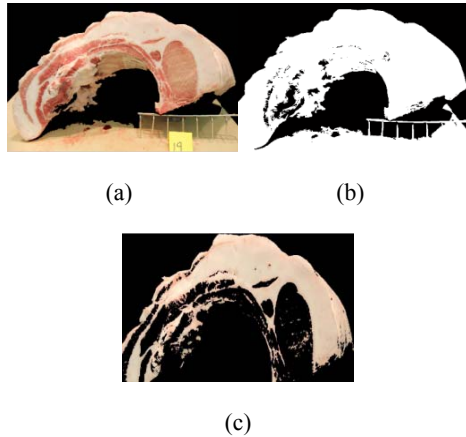


Fig.1: Segmentation of subcutaneous fat from a representative pork loin sample; (a): Original image; (b): Background segmentation; (c): Fat area

$$Iodine\ value = [C16:1] \times 0.95 + [C18:1] \times 0.86 + [C18:2] \times 1.732 + [C18:3] \times 2.616 + [C20:1] \times 0.785 + [C22:1] \times 0.723 \quad (1)$$

picnic shoulder were removed from the anterior section. The remaining rib section was placed against a black backdrop with the posterior (10th rib) facing the high resolution camera (Fig. 1). The outer dermis was removed from the loins; however, the full content of subcutaneous back fat remained for acquisition of photos and subsequent image analyses.

After image acquisition, a 40 g sample of subcutaneous fat was collected from the 10th rib section, frozen and sent to the University of Missouri Experiment Station Chemical Laboratories (Columbia, MO) for Fatty Acid Profile (FAP) analysis. Full FAP for saturated and mono- and polyunsaturated acids were performed using AOAC Official Method 996.06 (Analysis of Methyl Esters by Capillary GLC), AOCS Official Method Ce 2-66 (Preparation of Methyl Esters of Fatty Acids), AOAC Official Method 965.49 (Preparation of Methyl Esters of Fatty Acids) and AOAC Official Method 969.33 (oils and fat, GoronTriflouride method).

Image acquisition and processing: Pork loin images were acquired in the processing plant using a color digital camera (Model EOS 60D, Canon Corporation, Japan) with contrasting (black) background. Images were obtained in the plant to simulate the real-time industrial environment (Fig. 1a). Subsequent image analysis was conducted separately using image analyzing software (Matlab Version 7, The Mathworks, Natick, MA, USA).

Processing algorithms and analyses were developed to separate the subcutaneous fat area of interest from the background area using Matlab software. The color images were first segmented into background (dark) and loin sample (white) areas (Fig. 1b). After digital removal of the background, the color

threshold value was performed to separate the lean from the fat area (Fig. 1c). Each image was then saved as 860×598 pixel×8 bit.

Image texture features extraction: Five texture features (roughness, contrast, directionality, line-likeness and heterogeneity) were extracted from the images based on previous work by Tamura *et al.* (1978).

Roughness relates to distances of notable spatial variations of grey levels, that is, implicitly, to the size of the primitive elements (texels) forming the texture. The proposed computational procedure accounts for differences between the average signals for the non-overlapping windows of different size. Roughness, F_{rou} , can be computed as follows:

For image pixel area $2^k \times 2^k$, first calculate the average of the image grey value as:

$$A_k(x, y) = \sum_{i=x-2^{k-1}}^{x+2^{k-1}-1} \sum_{j=y-2^{k-1}}^{y+2^{k-1}-1} (g(i, j) / 2^{2k}) \quad (2)$$

where, $k = 0, 1, \dots, 5$; $g(i, j)$ is the pixel value of (i, j) . For each pixel, calculate the average intensity, E , of non-overlapping windows between the horizontal and vertical directions using:

$$E_{k,h}(x, y) = |A_k(x+2^{k-1}, y) - A_k(x-2^{k-1}, y)| \quad (3)$$

$$E_{k,v}(x, y) = |A_k(x, y+2^{k-1}) - A_k(x, y-2^{k-1})| \quad (4)$$

where, each image pixel allows to set up a value E , which reaches the maximum k to set the optimum size:

$$S_{best}(x, y) = 2^k \quad (5)$$

$$s.b. \max_{k=1}^{k_{max}} (E_{k,h}(x, y), E_{k,v}(x, y)) \quad (6)$$

In the end, the roughness equation can be calculated as:

$$F_{rou} = \frac{1}{m \times n} \sum_{x=1}^m \sum_{y=1}^n S_{best}(x, y) \quad (7)$$

Contrast: Measures the manner grey levels “q” vary in the image “I” and to what extent their distribution is biased to black or white. The second-order and normalized fourth-order central moments of the grey level histogram (empirical probability distribution), that is, the variance, σ^2 and kurtosis, α_4 , are used to define the contrast where contrast, F_{con} , can be computed as follows:

$$F_{con} = \sigma / (\alpha_4)^{0.25} \quad (8)$$

where,

$$\sigma^2 = (q-m)^2 \Pr(q|I)$$

$$\alpha_4 = 1/\sigma^4 \sum_{q=0}^{q_{max}} (q-m) \Pr(q|I)$$

Directionality is measured using the frequency distribution of oriented local edges against their directional angles. The edge strength, $e(x, y)$ and the directional angle, $a(x, y)$ are computed using the Sobel edge detector approximating the pixel-wisex- and y-derivatives of the image:

$$e(x, y) = 0.5(|\Delta_x(x, y)| + |\Delta_y(x, y)|) \quad (9)$$

$$a(x, y) = \tan^{-1}(\Delta_y(x, y)/\Delta_x(x, y)) \quad (10)$$

where, $\Delta_x(x, y)$ and $\Delta_y(x, y)$ are the horizontal and vertical grey level differences between the neighboring pixels, respectively. The differences are measured using the following 3×3 moving window operators:

$$\begin{matrix} -1 & 0 & 1 & 1 & 1 \\ -1 & 0 & 1 & 0 & 0 \\ -1 & 0 & 1 & -1 & -1 \end{matrix} \quad (11)$$

A histogram, $H_{dir}(a)$, of quantized direction values, a , is constructed by counting the number of the edge pixels with the corresponding directional angles and the edge strength greater than a predefined threshold. The histogram is relatively uniform for images without strong orientation and exhibits peaks for highly directional images. The degree of directionality relates to the sharpness of the peaks. Directionality, F_{dir} , can be computed as follows:

$$F_{dir} = 1 - m_{peaks} \sum_{p=1}^{n_{peaks}} \sum_{a \in w_p} (a - a_p)^2 H_{dir}(a) \quad (12)$$

The line-likeness feature, F_{lin} , is defined as an average coincidence of the edge directions (more precisely, coded directional angles) that co-occur in the pairs of pixels separated by a distance, d , along the edge direction in every pixel. Line-likeness, F_{lin} , can be computed as follows:

$$F_{lin} = \sum_i^n \sum_j^n P_{Dd}(i, j) \cos[(i-j) \frac{2\pi}{n}] / \sum_i^n \sum_j^n P_{Dd}(i, j) \quad (13)$$

Heterogeneity: Calculates the fraction of image pixels that is superior to the threshold value (10%) from the average intensity of the object. Image heterogeneity is defined by dividing the fat image feature into a window of size (n×m) and computing the window intensity mean on each window. Then, the texture of heterogeneous feature, F_{het} , can be computed as follows:

$$F_{het} = MI = \sum_{i=1}^n I(i) / S \quad (14)$$

where, $|MI[wi]-MI| > 10\%$; $I(i)$ is the intensity of pixel; and S is the number of pixels.

Fatty acid prediction using linear and stepwise regression methods: Linear regression analysis was established to predict the quantity of oleic, linoleic and linolenic fatty acids as well as IV using the five texture features (contrast, roughness, heterogeneity, line-likeness, directionality) in the model.

Step wise linear discrimination and regression analysis were used to determine the most likely predictors from the five texture features. Unlike the linear regression analysis, the stepwise discrimination method was first performed to select the useful texture features from the five texture features using statistical software (SPSS 20.0) setting the significance level value at 0.05 for inclusion and at 0.15 for exclusion from the prediction model.

RESULTS AND DISCUSSION

The image texture features of contrast, roughness, heterogeneity, line-likeness and directionality were successfully extracted from images of the intact subcutaneous fat adjacent to the longissimus lumborum muscle at the 10th thoracic vertebra. The image texture features were utilized in linear and stepwise regression models to predict percentages of total fat for oleic, linoleic and linolenic fatty acids and IV (Table 1). Ripoché and Guillard (2001) used near infrared reflectance spectroscopy to determine the fatty acid composition and the results showed promising regards the R² value (above 0.90). But compared to the digital image acquisition method, the infrared method need 1 minute to acquire each sample, that will lead some potential time consuming issues to the future fatty acid detection requirement.

González-Martín *et al.* (2005) used near infrared spectrometer and regression methods to predict porkloin fatty acid attributes (C14:0, C16:0, C16:1, C17:0, C17:1, C18:0, C18:1, C18:2, C18:3, Σ polyunsaturated, Σ monounsaturated and Σ saturated). The results showed the highest correlation coefficients were 0.943 (Σ monounsaturated). De Marchi *et al.* (2012) predicted chicken meat fatty acid characteristics using near infrared spectroscopy at line in slaughterhouse which will fit the industry speed requirement. Results showed low significant correlation coefficients value (less than 0.60) to predict the fatty acid composition of chicken meat. In this research, for all predictions, linear regression models had a higher R² than stepwise regression models. For oleic acid, the linear regression model had an R² of 0.86 while the stepwise regression model had an R² of 0.65. For linoleic and linolenic, both linear regression models

Table 1: Linear and stepwise regression model summary developed from color image texture features of pork subcutaneous fat

Control	Model	R	R ²	SEE ^c
Leic	Linear ^a	0.93	0.86	3.03
	Stepwise ^b	0.80	0.65	3.16
Linoleic	Linear ^a	0.98	0.95	3.33
	Stepwise ^b	0.90	0.80	4.45
Linolenic	Linear ^a	0.97	0.95	0.37
	Stepwise ^b	0.90	0.81	0.45
Iodine Value (IV)	Linear ^a	0.98	0.95	5.07
	Stepwise ^b	0.90	0.82	6.37

^aPredictors: (Constant), Directionality, Contrast, Roughness, Heterogeneity, Line-likeness, ^bPredictors: (Constant), Roughness, ^cSEE: Standard Error of the Estimate

resulted in an R² value of 0.95 while the stepwise regression R² values for linoleic and linolenic were 0.80 and 0.81, respectively. For IV, the linear regression model reached an R² of 0.95 while the stepwise regression only had an R² of 0.82. Due to the small sample size, no validation data was generated for the linear regression model.

Although the linear regression model produced effective results in this preliminary analysis, other analysis methods such as non-linear regression or artificial neural network should be investigated from a larger population of pork samples possessing more variability in fatty acid profile and subsequent fat quality.

CONCLUSION

This research shows the potential for the extraction of image texture features from pork loin images obtained in a processing plant environment as a means for quantifying fatty acids known to influence processing attributes of pork fat. From the satisfied results in this research, it showed imaging technology has significant ability of suitable the prerequisite of industry online application.

ACKNOWLEDGMENT

This research was supported by Natural Science Foundation of Jiangsu Province (award no. BK20140715).

REFERENCES

AOCS, 1998. Method Cd 3b-76: Saponification Value. In: Firestone, D. (Ed.), Official Methods and Recommended Practices of the American Oil Chemists' Society, 5th Edn., American Oil Chemists' Society, Champaign, Illinois, USA.

Chandraratne, M.R., D. Kulasiri, C. Frampton, S. Samarasinghe and R. Bickerstaffe, 2006a. Prediction of lamb carcass grades using features extracted from lamb chop images. *J. Food Eng.*, 74(1): 116-124.

Chandraratne, M.R., S. Samarasinghe, D. Kulasiri and R. Bickerstaffe, 2006b. Prediction of lamb tenderness using image surface texture features. *J. Food Eng.*, 77(3): 492-499.

Chandraratne, M.R., D. Kulasiri and S. Samarasinghe, 2007. Classification of lamb carcass using machine vision: Comparison of statistical and neural network analyses. *J. Food Eng.*, 82(1): 26-34.

Chen, K., X. Sun, C. Qin and X. Tang, 2010. Color grading of beef fat by using computer vision and support vector machine. *Comput. Electron. Agr.*, 70(1): 27-32.

Chmiel, M., M. Słowiński and K. Dasiewicz, 2011a. Lightness of the color measured by computer image analysis as a factor for assessing the quality of pork meat. *Meat Sci.*, 88(3): 566-570.

Chmiel, M., M. Słowiński and K. Dasiewicz, 2011b. Application of computer vision systems for estimation of fat content in poultry meat. *Food Control*, 22(8): 1424-1427.

De Marchi, M., R. Riovanto, M. Penasa and M. Cassandro, 2012. At-line prediction of fatty acid profile in chicken breast using near infrared reflectance spectroscopy. *Meat Sci.*, 90(3): 653-657.

Girolami, A., F. Napolitano, D. Faraone and A. Braghieri, 2013. Measurement of meat color using a computer vision system. *Meat Sci.*, 93(1): 111-118.

González-Martín, I., C. González-Pérez, N. Alvarez-García and J.M. González-Cabrera, 2005. On-line determination of fatty acid composition in intramuscular fat of Iberian pork loin by NIRs with a remote reflectance fibre optic probe. *Meat Sci.*, 69(2): 243-248.

Hallenstvedt, E., M. Øverland, A. Rehnberg, N.P. Kjos and M. Thomassen, 2012. Sensory quality of short- and long-term frozen stored pork products. Influence of diets varying in polyunsaturated fatty acid (PUFA) content and iodine value. *Meat Sci.*, 90(1): 244-251.

Ripoche, A. and A.S. Guillard, 2001. Determination of fatty acid composition of pork fat by Fourier transform infrared spectroscopy. *Meat Sci.*, 58(3): 299-304.

Sun, X., K.J. Chen, K.R. Maddock-Carlin, V.L. Anderson, A.N. Lepper *et al.*, 2012. Predicting beef tenderness using color and multispectral image texture features. *Meat Sci.*, 92(4): 386-393.

Sun, X., K.J. Chen, E.P. Berg, D.J. Newman, C.A. Schwartz *et al.*, 2014. Prediction of troponin-T degradation using color image texture features in 10d aged beef longissimus steaks. *Meat Sci.*, 96(2 Pt A): 837-842.

Tamura, H., S. Mori and T. Yamawaki, 1978. Textural features corresponding to visual perception. *IEEE T. Syst. Man Cyb.*, 8(6): 460-473.